Title
Atmospheric chemistry of an Antarctic volcanic plume

Journal
Journal of Geophysical Research, 115(D4)

ISSN
0148-0227

Authors
Oppenheimer, Clive
Kyle, Philip
Eisele, Fred
et al.

Publication Date
2010-02-27

DOI
10.1029/2009jd011910

JOURNAL OF GEOPHYSICAL RESEARCH, VOL. 115, D04303, doi:10.1029/2009JD011910, 2010

Atmospheric chemistry of an Antarctic volcanic plume

Clive Oppenheimer,[1] Philip Kyle,[2] Fred Eisele,[3] Jim Crawford,[4] Greg Huey,[5]
David Tanner,[5] Saewung Kim,[5] Lee Mauldin,[3] Don Blake,[6] Andreas Beyersdorf,[6,7]
Martin Buhr,[8] and Doug Davis[5]

Received 12 February 2009; revised 15 September 2009; accepted 22 September 2009; published 27 February 2010.

[1] We report measurements of the atmospheric plume emitted by Erebus volcano, Antarctica, renowned for its persistent lava lake. The observations were made in December 2005 both at source, with an infrared spectrometer sited on the crater rim, and up to 56 km downwind, using a Twin Otter aircraft; with the two different measurement platforms, plume ages were sampled ranging from <1 min to as long as 9 h. Three species (CO, carbonyl sulfide (OCS), and SO_2) were measured from both air and ground. While CO and OCS were conserved in the plume, consistent with their long atmospheric lifetimes, the downwind measurements indicate a SO_2/CO ratio about 20% of that observed at the crater rim, suggesting rapid chemical conversion of SO_2. The aircraft measurements also identify volcanogenic H_2SO_4, HNO_3 and, recognized for the first time in a volcanic plume, HO_2NO_2. We did not find NO_x in the downwind plume despite previous detection of NO_2 above the crater. This suggests that near-source NO_x was quickly oxidized to HNO_3 and HO_2NO_2, and probably $NO^{2-}_{3\,(aq)}$, possibly in tandem with the conversion of SO_2 to sulfate. These fast processes may have been facilitated by "cloud processing" in the dense plume immediately downwind from the crater. A further striking observation was O_3 depletion of up to ∼35% in parts of the downwind plume. This is likely to be due to the presence of reactive halogens (BrO and ClO) formed through heterogeneous processes in the young plume. Our analysis adds to the growing evidence for the tropospheric reactivity of volcanic plumes and shows that Erebus volcano has a significant impact on Antarctic atmospheric chemistry, at least locally in the Southern Ross Sea area.

Citation: Oppenheimer, C., et al. (2010), Atmospheric chemistry of an Antarctic volcanic plume, *J. Geophys. Res.*, *115*, D04303, doi:10.1029/2009JD011910.

1. Introduction

[2] An important finding concerning the impact of global volcanism is the disproportionately high contribution of sulfate loading in the atmosphere due to sulfur emissions from nonexplosive, degassing volcanoes compared with other sulfur sources, including anthropogenic and oceanic emissions [e.g., *Chin and Jacob*, 1996; *Graf et al.*, 1997; *Stevenson et al.*, 2003]. This partly reflects the elevation of volcanic sources, which leads to enhanced atmospheric residence times for volcanic sulfur gases and aerosols compared with many oceanic or anthropogenic sources. Thus, the temporal and spatial variability in this "background" volcanic source may represent an important climate forcing factor that has yet to be fully characterized. In addition to the impacts from sulfur compounds, there is further evidence of enhanced atmospheric chemical reactivity induced by volcanic plumes due to the presence of reactive halogens [e.g., *Bobrowski et al.*, 2003, 2007; *Bobrowski and Platt*, 2007; *Oppenheimer et al.*, 2006; *Theys et al.*, 2009; *Roberts et al.*, 2009] and nitrogen species [e.g., *Huebert et al.*, 1999; *Mather et al.*, 2004a, 2004b; *Martin et al.*, 2006]. In light of these findings, it is likely that, at least on a local scale, volcanic plumes strongly perturb tropospheric acidity and oxidizing capacity.

[3] Here we report airborne and ground-based measurements of Antarctica's most persistently active volcano, Mount Erebus (77° 32′S, 167° 10′E, 3794 m above sea level). The observations were made under the auspices of the Antarctic Tropospheric Chemical Investigation (ANTCI) 2005 project (http://acd.ucar.edu/∼mauldin/ANTCI_Web/ANTCI_Home.htm) and the research program of the Mount Erebus Volcano Observatory (http://erebus.nmt.edu/). The primary motivation for our focus on Erebus was to investigate peculiarities in volcanic plume chemistry that might be associated with the characteristics of the Antarctic atmosphere, and, more specifically, to improve our understanding

---

[1] Department of Geography, University of Cambridge, Cambridge, UK.

[2] Department of Earth and Environmental Science, New Mexico Institute of Mining and Technology, Socorro, New Mexico, USA.

[3] Atmospheric Chemistry Division, National Center for Atmospheric Research, Boulder, Colorado, USA.

[4] NASA Langley Research Center, Hampton, Virginia, USA.

[5] School of Earth and Atmospheric Sciences, Georgia Institute of Technology, Atlanta, Georgia, USA.

[6] Department of Chemistry, University of California, Irvine, California, USA.

[7] Now at NASA Langley Research Center, Hampton, Virginia, USA.

[8] Air Quality Design, Inc., Golden, Colorado, USA.

0148-0227/10/2009JD011910$09.00

of NO_x chemistry in volcanic plumes following previous observations of NO_2 emissions above the Erebus crater [*Oppenheimer et al.*, 2005]. This NO_2 was thought to have been formed from oxidation of atmospheric N_2 at the hot surface of the volcano's active lava lake. It was also suggested that Erebus represents the largest point source of NO_x in Antarctica, and that the emission might be relevant to understanding highly elevated levels of NO (>0.6 ppbv) observed occasionally in near surface air at South Pole [*Davis et al.*, 2001, 2004, 2008].

[4] Prior studies of the Erebus plume using instrumented aircraft include those of *Radke* [1982], *Rose et al.* [1985], *Chuan et al.* [1986], and *Chuan* [1994]. *Radke* [1982] reported the results of several research flights carried out in mid-November 1980. He found that most of the plume aerosol mass was narrowly confined to particles with diameter of ~100 nm, suggesting a single mechanism involved in aerosol production operating close to the crater. He pointed out that particles of such a size (corresponding to the so-called "Greenfield gap") should be exceptionally long-lived due to minimum scavenging efficiency, and suggested that up to 32% of the Antarctic total sulfate budget could be sourced by Erebus alone. Based on plume sampling at the crater, *Zreda-Gostynska et al.* [1997] confirmed the volcano's strong emission of many species including halogens and trace metals leading them to suggest Erebus might contribute up to 80% of the Cl deposited at South Pole.

[5] *Shaw* [1983] tentatively identified Erebus aerosol at South Pole on the basis of Cl and Si content, while *Arimoto et al.* [2004a, 2004b] suggested the volcano contributes to sulfate and trace metals in South Pole aerosol. *Chuan* [1994] also argued for long-range transport of Erebus aerosol across the Polar Plateau, at least as far south as latitude 88.7°S, based on airborne collection of particles containing diagnostic Au and KCl. *Vallelonga et al.* [2003] also considered Erebus as the origin of trace metal peaks in the glaciochemistry of ice cores drilled at Law Dome, Wilkes Land (~2000 km from Erebus). More recently, *Shirsat and Graf* [2009] demonstrated the preeminence of Erebus' contribution to the Antarctic atmospheric SO_2 budget, based on an inventory of natural and anthropogenic sources. *Graf et al.* [2009] used this inventory (which excludes DMS) in a limited area chemistry climate model to suggest that Erebus contributes around 10 pptv to the tropospheric SO_2 burden in the Ross Sea region and is a significant source of sulfate deposition on the Royal Society mountain range.

[6] The new measurements we report here were made both by tracking the plume downwind using an instrumented aircraft, and at the summit crater using a Fourier transform infrared (FTIR) spectrometer sited on the crater rim. We were thus able to characterize several aspects of the chemical evolution of the Erebus plume as it drifted for an estimated 9 h in the troposphere (at a height of ~3800 m above sea level). Specific aims included an assessment of the nitrogen and sulfur chemistry of the plume, with an emphasis on contrasting the gas phase composition of the very young plume (in the crater) with the aged plume drifting downwind.

2. Methods

2.1. Airborne Measurements

[7] Measurements were made on two flights (8 and 9, introduced in section 2.2) of an instrumented DHC-6 Twin Otter aircraft for the following chemical species: NO, HNO_3, HO_2NO_2, SO_2, COS, CO, O_3 and H_2O. More limited observations were also available during flight 9 for H_2SO_4 and OH. In all cases, air intakes for the sampling lines were located forward of the aircraft engines, and outside of the fuselage boundary layer. Controlled tests in which NO from an on-board tank was released next to the aircraft skin at different positions excluded the possibility of contamination from the cabin. In addition, flight tests were carried out in which NO was monitored while the aircraft was put through different flight maneuvers. These established that, while flying horizontally, no exhaust from the aircraft engines reached the sampling system. This was also the case for tests involving vertical spirals in which descent rates of 150 m min^{-1} were maintained. The only flight mode in which engine exhausts were occasionally detected was when the aircraft flight track involved tight 180° or 360° turns. The worst case scenario was when the aircraft made a 180° turn, followed by repositioning itself downwind of its point of passage through the plume. As indicated later in the text, this flight pattern did occasionally result in sampling of engine generated NO.

[8] The detection limit, 2σ random error, and the calibration uncertainty for each of the critical species measured from the aircraft are given in Table 1. The detection limit reported is typically based on a 1 min integration time. (Note that during ground-based studies the integration time can be increased by factors of 5 to 20, thus further enhancing the stated detection limit for a species.) The cited calibration uncertainty represents the maximum potential systematic error in the airborne measurements based on calibration standards. In most cases (H_2SO_4 being the exception) the potential systematic error was $\leq$20% of the measured value.

[9] Measurements of NO were made using a chemiluminescence technique. This methodology has been well-established through instrument intercomparison studies involving both airborne and ground-based sampling platforms [e.g., *Hoell et al.*, 1987; *Gregory et al.*, 1990]. The NO system was calibrated using a standard addition methodology, which was performed at least twice per flight (for additional details, see also *Davis et al.* [2001, 2004, 2008]). Measurements of O_3 were made using a commercial UV absorption instrument, which again has undergone numerous field tests, and is a well-proven instrument [*Gregory et al.*, 1983]. Both the random and potential systematic errors in the measurements are given in Table 1.

[10] Measurements of SO_2, HNO_3, HO_2NO_2 and H_2SO_4 involved two versions of the select ion chemical ionization mass spectrometry technique. For SO_2, HNO_3 and HO_2NO_2, sampling was achieved through a heated inlet that extended ~0.5 m from the aircraft skin. The sampling line itself was made of 1/2 inch OD Teflon tubing, approximately 2.6 m in total length. The reagent ion used to detect SO_2, HNO_3 and HO_2NO_2 was SF_6^-, which was generated in an ion source chamber by associative electron capture. A typical measurement sequence consisted of integrating the signal at 148 amu ($^{34}SF_6^-$) for 25 ms, 82 amu ($NO_3^- \cdot HF$) for 2 s, 98 amu ($NO_4^- \cdot HF$) for 2 s, and 102 amu ($F_2SO_2^-$) for 0.5 s. Background measurements were collected every few minutes by diverting ambient flow through a filter containing nylon wool and activated charcoal. Typical

Table 1. Chemical Species Detection Limits and Measurement Uncertainties

Chemical Species	Detection Limit[a]	Random Error (2σ)[b] (%)	Calibration Uncertainty[c] (%)
CO	10 ppbv	5	10
OCS	10 pptv	5	15
NO	4 pptv	10	10
HNO_3	5 pptv	27	20
HO_2NO_2	5 pptv	24	20
SO_2	5 pptv	15	20
H_2SO_4	5×10^5 molecule cm^{-3}	20	40
O_3	2 ppbv	3	5

[a] Detection limit (DL) for S/N = 2.0.
[b] Two-sigma error when signal ≥ 5 × DL.
[c] Percent of measured value.

sensitivities obtained for HNO_3 and SO_2 during the field study were 7 and 4 counts per second (parts per trillion by volume)$^{-1}$, respectively [see *Huey et al.*, 1995, 2004; *Slusher et al.*, 2001]. Note, for the latter instrument, we also considered a further potential systematic error not cited in Table 1 arising from the specific configuration employed during the ANTCI 2005 study. This is the slight possibility that an interference ion of nearly the same mass as that produced from HNO_3 could have been generated when SO_2 levels were very high (>10 ppbv). However, that this potential error was small (≤0.5% of the measured value of SO_2) is strongly suggested from an examination of a subset of the HNO_3 and SO_2 data corresponding to lower plume abundances (up to SO_2 mixing ratios of 2 ppbv). Figure 1 displays these screened data and indicates a number of data pairs where SO_2 abundance ranges from background values (≤0.01 ppbv) up to ~2 ppbv but for which HNO_3 is as low as 0.005 ppbv. These data clearly suggest a significant degree of heterogeneity in the plume, but more importantly, they show that there is no increasing trend evident in HNO_3 levels with increasing SO_2 up to ~2 ppbv. Further evidence for very limited interference is that between 2 and 10 ppbv of SO_2, the trend in data pairs in Figure 1 is consistent with the trend for the entire data set, which extends to SO_2 abundances in excess of 30 ppbv. Notwithstanding these comments, all plume HNO_3 measurements still should be viewed as upper limit values.

[11] A final point regarding the sampling of both SO_2 and HNO_3 involves the small but persistent "tailing effect" seen on the larger peaks, especially those for SO_2. Although some of this tailing effect may have been the result of the

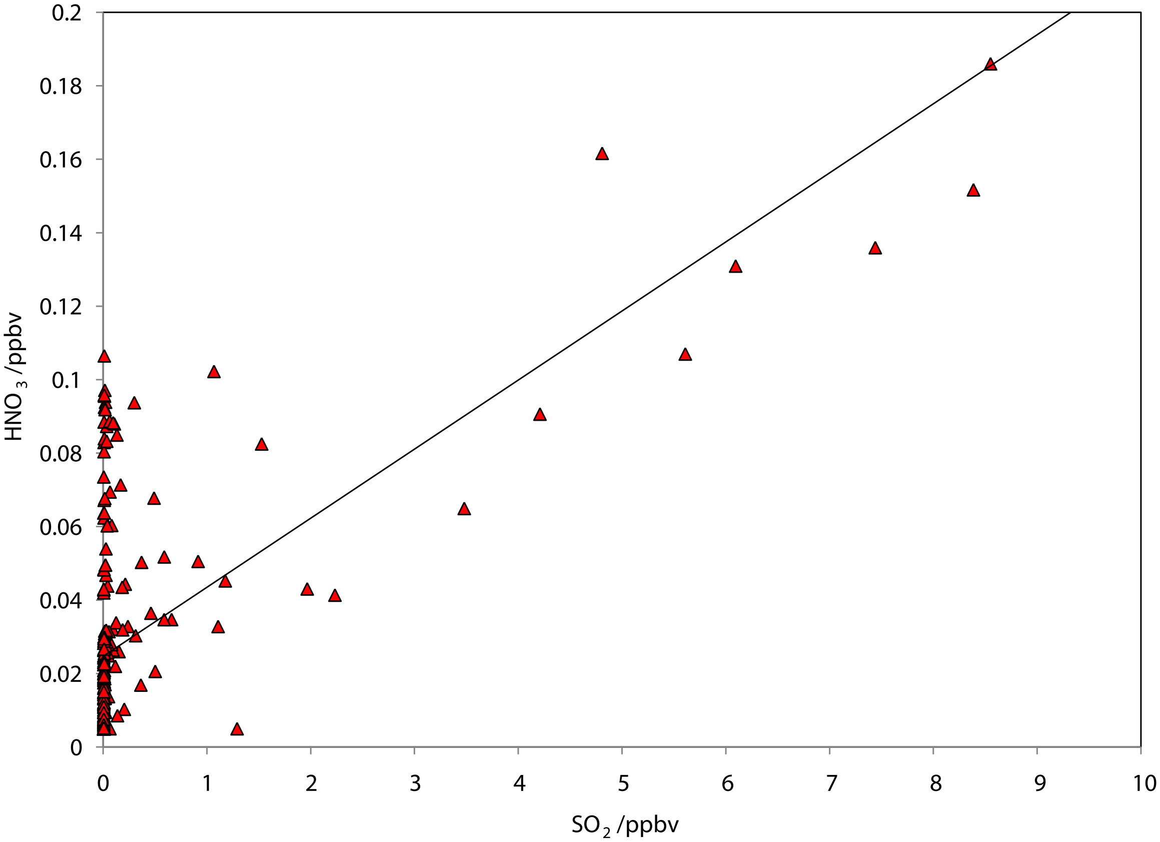

Figure 1. SO_2 and HNO_3 observations from research flights carried out on 9 and 11 December 2005 in vicinity of Erebus volcano, showing only data pairs for which SO_2 levels were below 10 ppbv. The lack of any trend in HNO_3 versus SO_2 for SO_2 < 2 ppbv, the few high values of SO_2 that are not matched by comparably high HNO_3 levels, and the clear trend in SO_2 versus HNO_3 between 2 and 10 ppbv of SO_2 (which is related to the visible volcanic plume) all point to negligible interference of SO_2 on the HNO_3 measurements. The line indicates the linear regression through all the SO_2 and HNO_3 observations for both flights (including the data points for concentrated plume not shown in this graph). See also Figure 6.

Table 2. Timing, Location, and Meteorology for Plume Intercepts by Aircraft

Flight Number	Plume Intercept Time (UTC)	Local Time	Distance to Crater (km)	Maximum Plume Age (h)	Solar Elevation	Flight Altitude Above Sea Level (m)	Air Temperature (K)	Dew Point (K)	Wind Speed ($m\ s^{-1}$)
8	0450–0600, 9 December 2005	1750–1900	4–20	~2	21°–25°	~3815	248–251	246–249	3.1
9	2230–2310, 10 December 2005	1130–1210 (11 December)	1–56	~9	33°–34°	~3815	246–251	not available	1.8

stickiness of these compounds and the need to use longer sampling lines, most of it is likely related to a background shift in the instrument upon entering the densest volcanic gas/aerosol areas of the plume. Though, in principle, this affect could have been removed by rezeroing the instrument while in the plume, this was not practical under the sampling conditions presented by the Erebus plume. Most importantly, this perturbation was quite small when compared to the real signal while in the plume, and it had no significant influence on the interpretation of the data.

[12] In the measurement of H_2SO_4 and OH the reagent ion employed was NO_3^-, which was generated in an ion source where the air stream had HNO_3 injected into it. The detection of OH involved first allowing ambient OH in the sampled gas stream to react with $^{34}SO_2$ to form $^{34}SO_3$. This product was then allowed to react with H_2O in the gas stream, forming $H_2^{34}SO_4$. After reaction with the reagent ion NO_3^-, the final detected ion was $H^{34}SO_4^-$. Thus, both ambient H_2SO_4 as well as OH were ultimately measured mass spectrometrically via the detection of the HSO_4^- ion [see *Tanner et al.*, 1997; *Mauldin et al.*, 1998, 2004]. Unfortunately, due to instrument difficulties, OH abundance could only be evaluated semiquantitatively, based on measurements from a later ANTCI flight.

2.2. Airborne Plume Intercept Details

[13] The Erebus plume was intercepted between 4 and 20 km from the crater at ~0450–0600 UTC on 9 December 2005 (flight 8), and between 1 and 56 km from the crater at ~2230–2310 UTC on 10 December 2005 (flight 9). These distances correspond to an estimated plume age that ranges from 30 min to 2 h for flight 8, and from 10 min to nearly 9 h for flight 9. These age estimates are based on wind speed estimates from two rawinsonde launches at McMurdo Station (~35 km away) for the altitude of the plume. For flights 8 and 9 these were 3.1 and 1.8 m s^{-1}, respectively. However, it should be borne in mind that the time of the rawinsonde launches at McMurdo was several hours removed from the actual flight times. Thus, changes in wind speed and direction both before the rawinsonde launch as well as during the course of each plume study cannot be ruled out. Postanalyses of the meteorological wind fields in the immediate vicinity of Erebus volcano in the form of forward air trajectories (based on Polar MM5 modeling results) suggest that, in the very early morning hours, winds were very light and highly variable in direction. In addition, when using these wind speed data as a 'clock' for estimating the advection of the plume core, and hence, for estimating the chemical reaction time in the plume, it must be recognized that these data cannot provide a good guide to time scales of cross-wind plume mixing. In the latter case, different degrees of chemical processing can be encountered at different locations within the plume (different points along a radial axis reflecting the extent of dilution) even though the distance from the crater rim is the same for all points along the axis. (Note that a sampling integration time of 1 min corresponds to about 4 km of flight at the mean ground speed of ~250 km h^{-1} which means that considerable spatial averaging of the abundances of species occurs each time the aircraft crosses the plume.)

[14] Antarctic local time was the same as New Zealand Daylight Time (UTC+13 h); thus the encounters occurred at 1750–1910 (9 December) and 1130–1210 (11 December) local time. Table 2 lists the relevant environmental and geographical data pertaining to the plume encounters. The photograph in Figure 2 illustrates the high degree of plume visibility on 11 December (as seen from ~25 km away) and thus reflects the stable atmospheric conditions prevailing around the time of takeoff for flight 9. Plume visibility was significantly lower during flight 8.

2.3. Ground-Based Measurements

[15] Measurements at the crater rim of Erebus were made using a portable FTIR spectrometer (MIDAC M-4402-1) fitted with ZnSe beam splitter and a liquid nitrogen-cooled

Figure 2. Photograph of Erebus volcano and its plume shortly before flight 9 on 11 December 2005. The plume was readily visible with the naked eye from a distance of ~25 km. Note the especially dense plume phase that stretches several kilometers downwind from the crater. Note also that for this time of year in Antarctica, significant actinic flux is present 24 h a day although there is a modest diurnal variation. Photograph taken by Jim Crawford.

InSb detector. Seven volcanic species were determined: H_2O, CO_2, CO, SO_2, HCl, HF and OCS. The instrument's 10 inch Newtonian telescope (field of view of 3 mrad) was trained on the active lava lake (the IR source), such that the plume was sampled within seconds or a few tens of seconds after release into the atmosphere along a path of ~300 m from the crater rim to the lava surface. All spectra were recorded with a nominal optical path difference (retardation) of 2.0 cm, corresponding to ~0.5 cm^{-1} spectral resolution. Consecutive batches of 8 interferograms were averaged (i.e., 8 sweeps of the mirror, which took ~8 s) to enhance the signal.

[16] The resulting interferograms were inverse Fourier transformed with a Mertz phase correction and triangular apodization, and the resulting single-beam spectra were analyzed by simulating the atmospheric transmittance in several discrete 'microwindow' wave bands [e.g., *Oppenheimer et al.*, 1998; *Burton et al.*, 2000; *Horrocks et al.*, 2001] using the Reference Forward Model [*Edwards and Dudhia*, 1996] and line parameters from the HITRAN database [*Rothman et al.*, 2005] for required gas species. The model considers a one-layer atmosphere with pressure, temperature and initial column amounts specified for both atmospheric and volcanic gas species. A second-order polynomial was also computed to detrend the local slope of the spectrum. The simulated spectra were adjusted to fit each observed spectrum using an optimal estimation method [*Rodgers*, 1976]. Relative errors were computed for each of the fitted components in the retrieval procedure based on the standard deviation of the residual (equal to the forward model minus the measurement), and, for our measurements, lie mostly in the range of 5–10% (see also *Horrocks et al.* [2001] for discussion of error budgets for the method). Molar abundance ratios were computed for pairs of gas species by simple, unweighted regression of the set of retrieved column amounts. Further details of the application of open-path FTIR spectroscopy on Erebus are given by *Oppenheimer and Kyle* [2008] and *Oppenheimer et al.* [2009].

[17] The FTIR measurements began on 12 December 2005, 24 h after flight 9 and it is the retrievals of this first data set that we present here. We note that our FTIR measurements throughout the 2005/2006 austral summer field season demonstrate that the plume composition varies little over time scales of a few weeks. Thus we are very confident that the intracrater plume composition recorded by FTIR spectroscopy provides a suitable comparison for the airborne in-plume data obtained in the preceding days.

3. Results

[18] Of the species measured during the Twin Otter flights, several showed enhancements in the volcanic plume. We report first the observations of the magmatic gases, then results for NO_y and O_3. Measurements were also made for a number of organic species but none showed significant perturbations in their concentrations in the plume, and we do not therefore discuss them further.

3.1. SO_2, CO, OCS, and H_2SO_4

[19] The SO_2 observations, because of their highly elevated levels, provided one of more reliable indicators of the plume core. Thus, these data suggest that the emissions from Erebus were sampled in excess of 50 km downwind of the crater (Figure 3). The highest SO_2 mixing ratios, up to 30 ppbv, were measured on flight 9. However, as much as 0.238 ppbv of SO_2 was detected at ~56 km from the crater, an abundance that was ~25–50 times background values (~0.005–0.010 ppbv). Of great interest, ANTCI flight 10 also encountered evidence of the Erebus plume while sampling above the Polar Plateau on 12 December 2005, a distance of ~600 km from the volcanic source [*Slusher et al.*, 2010]. During this mission, the aircraft flew from McMurdo to the automatic weather station at Mid-Point (75°S, 145°E). The plume was recognized by increases in both HNO_3 and SO_2. The former species reached levels that were ~0.06 ppbv above background; whereas SO_2 was 0.005–0.01 ppbv above stable background levels. Confirming the SO_2 results, there were corresponding elevations in H_2SO_4 levels. Further analyses of these data based on forward trajectory modeling confirmed Erebus as the most likely source and that the plume had been airborne for around 3–4 days by the time it was sampled.

[20] In clear association with SO_2, we find elevated gas phase H_2SO_4 in the plume encounters for flight 9 (Figure 4). The molar ratio of SO_2/H_2SO_4 is $\sim 4.1 \times 10^4$. However, there is also variability in the proportions of the two species, notably several samples with much higher H_2SO_4 relative to SO_2. These results reflect our earlier discussion pointing to the fact that the Erebus plume during this field study cannot be viewed as homogeneously mixed, and that radial mixing can lead to a rather complex chemical picture.

[21] Two other volcanic species, CO and OCS, which have been previously observed in the summit plume [*Oppenheimer and Kyle*, 2008] were also detected during the airborne measurements (Figure 5). The molar ratio of CO to OCS of ~300 is strikingly similar for both the airborne measurements and the summit FTIR observations. On the other hand, the SO_2/CO proportions for gas within the crater and distal plume differ markedly: the SO_2/CO molar ratio was ~0.42 at the source compared with ~0.082 downwind. Accepting comparability of the two techniques, this suggests significant depletion of SO_2 in the plume during advection. Also of note in the aircraft data, the observations for CO versus OCS are more strongly correlated than those for CO versus SO_2 ($r^2 = 0.99$ versus $r^2 = 0.78$, respectively).

[22] The molar abundance of CO in the magmatic gas is ~2% [*Oppenheimer and Kyle*, 2008] so the CO maxima observed in the downwind plume (~200–350 ppbv) correspond to a dilution of the plume by ambient air on the order of $1{:}10^4$ to $1{:}10^5$. For comparison, the mixing ratio of CO at the rim of the summit crater is already as low as 1–10 ppmv (i.e., diluted by ambient air within the crater in proportions of around $1{:}10^3$ to $1{:}10^4$), so the maximum CO abundance detected downwind corresponds to a further dilution of the plume (as sampled) by a factor of 10 to 100 after leaving the crater area. However, it must be borne in mind that the sampling time in flight corresponded to a cross-wind distance of ~4 km, thus there was the potential for sampling in and out of the plume during an individual measurement.

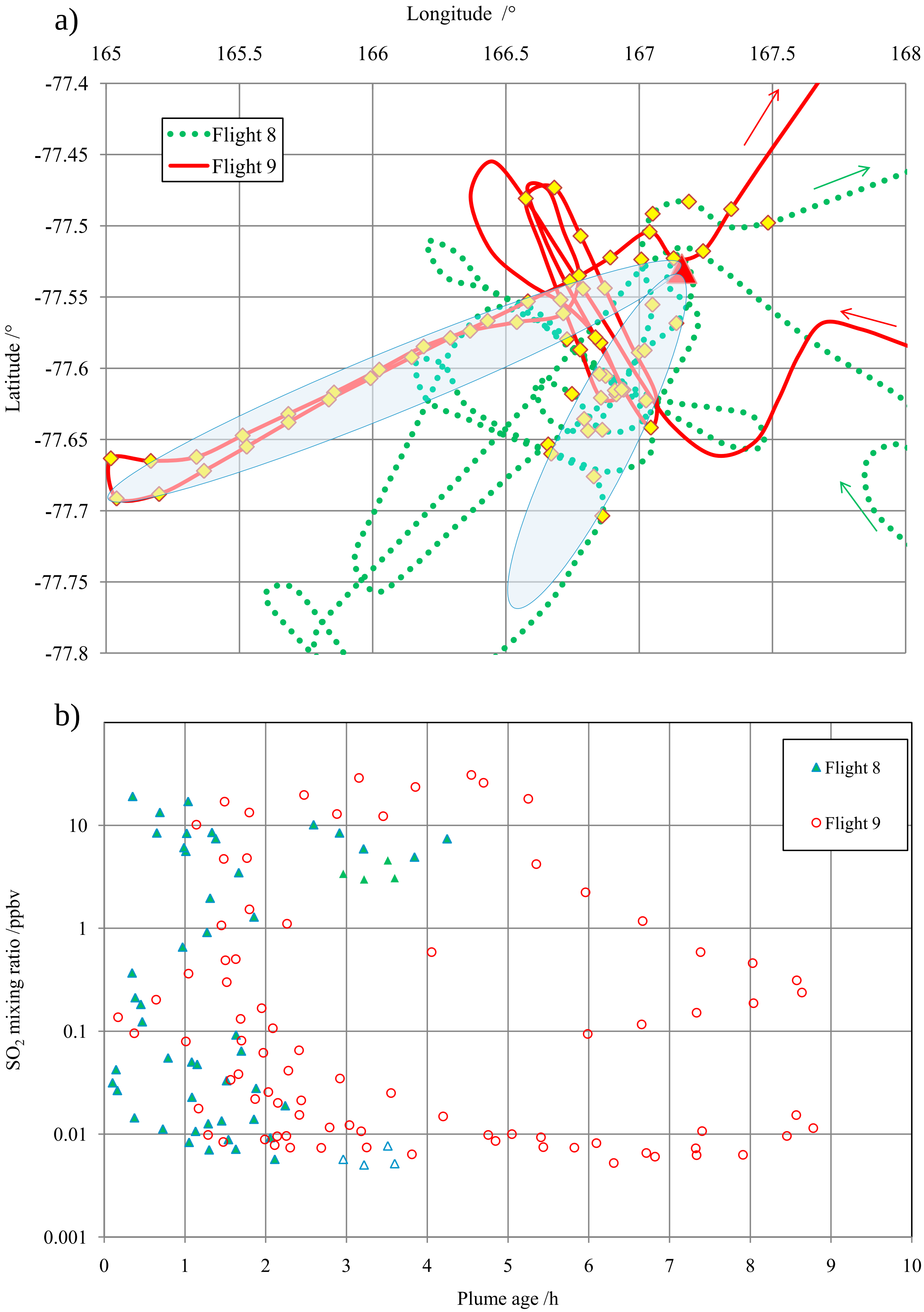
a)
Longitude /°
165
165.5
166
166.5
167
167.5
168
-77.4
-77.45
-77.5
-77.55
-77.6
-77.65
-77.7
-77.75
-77.8
Latitude /°
Flight 8
Flight 9
b)
Flight 8
Flight 9
SO$_2$ mixing ratio /ppbv
10
1
0.1
0.01
0.001
0
1
2
3
4
5
6
7
8
9
10
Plume age /h

Figure 3

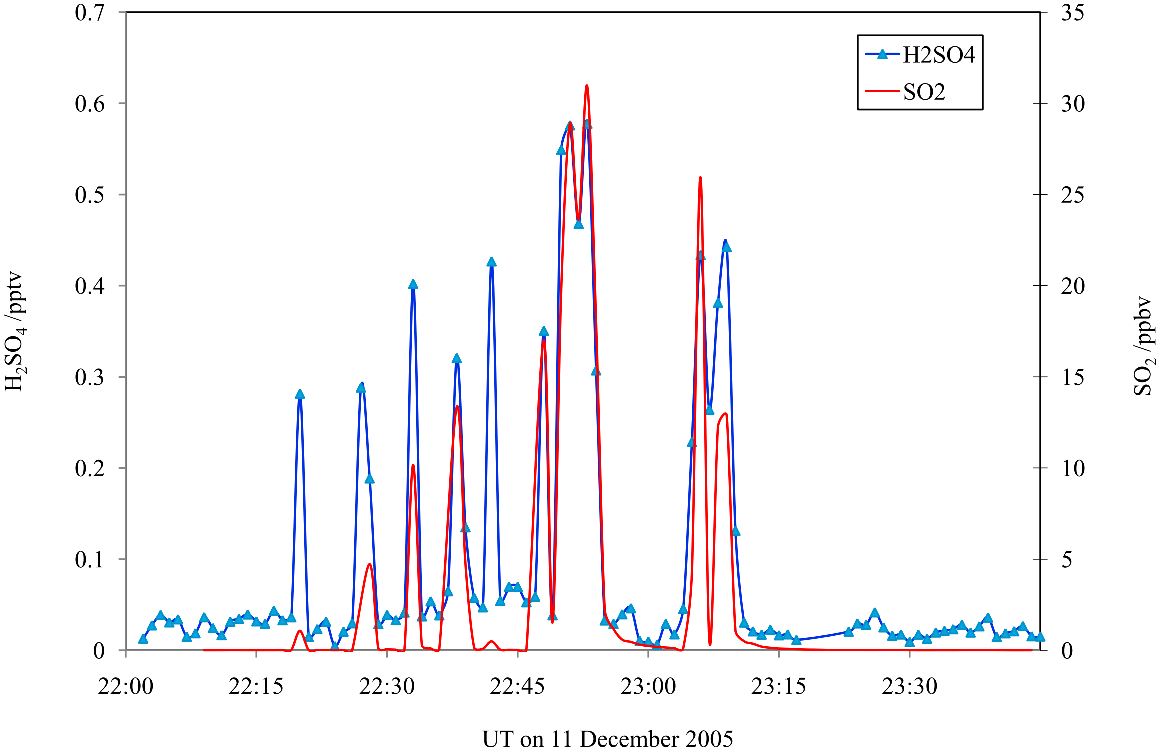

Figure 4. Observations from flight 9 on 11 December showing correspondence between SO_2 (red line) and H_2SO_4 (blue line with triangles) mixing ratios. Note different units (pptv for H_2SO_4 and ppbv for SO_2).

3.2. Volcanogenic NO_y

[23] The first notable finding for plume NO_y chemistry was the detection of HNO_3. Figure 6a shows the corresponding SO_2 and HNO_3 mixing ratios measured during flight 9: the SO_2/HNO_3 molar ratio is ∼56. The two species are strongly correlated (e.g., $r^2 > 0.9$), as shown in Figure 6b, with very similar results for both flights 8 and 9. Since HNO_3 is not a primary volcanic species we consider that its abundance reflects the atmospheric chemistry of the volcanic plume. But also of note during flight 9 is the long-wavelength "whaleback" profile in the measured HNO_3, which peaks at ∼0.1 ppbv around 2220 UTC (Figure 6a). This is a peculiar feature characterized by HNO_3 values generally >0.03 ppbv, which, from inspection of the flight lines, extends up to 15 km upwind from Erebus, and throughout the 56 km flight downwind. It is clearly independent of the spikes in HNO_3 that correspond to the visible crater plume (Figure 2). As also discussed above, significant evidence was found for the Erebus plume also reaching the Polar Plateau above which the HNO_3 levels observed were 0.060 ppbv above background levels (which were ∼0.040 ppbv).

[24] The other species with a clear plume signal is HO_2NO_2 (which was measured on flight 9 only). The peak in its mixing ratio is ∼0.13 ppbv (Figure 6b). The HO_2NO_2/HNO_3 molar ratio is ∼0.6, and the $SO_2/[HNO_3 + HO_2NO_2]$ ratio is ∼40. However, there was no evidence for volcanogenic NO_x in the plume based on the NO measurements. Although spikes in the NO concentration up to ∼0.08 ppbv were recorded, inspection of the GPS track indicates these can all be attributed to aircraft engine exhaust reaching the sampling line as a result of 180° turns.

3.3. Impacts of Erebus Plume on Ozone Abundance

[25] Ozone levels recorded during flight 9 reveal significant perturbations associated with the plume. These were particularly noticeable when the comeasured SO_2 abundance reached its highest values (Figure 7). This can be seen best at 2306 UTC when the SO_2 mixing ratio exceeds 25 ppbv and O_3 falls from a mean of $\sim 23.6 \pm 2.0$ (1σ) ppbv to a low of 14.8 ppbv (i.e., more than 4σ below the mean).

Figure 3. (a) Flight lines from GPS record; arrows show flight entries and exits. Erebus is the red triangle; flights 8 and 9 are indicated by dotted green and solid red lines, respectively. Yellow diamonds indicate observed SO_2 mixing ratios above 0.05 ppbv. Using this as a plume discriminator, the emissions have been tracked up to 56 km from source. The gray ovals indicate very approximately the location of the plume during the two encounters. (b) SO_2 mixing ratios observed during flights 8 (green triangles) and 9 (red circles) plotted as a function of plume age (estimated from an early morning wind speed observation for the approximate altitude of the Erebus plume taken from one rawinsonde observation at McMurdo). During flight 8, the plume became virtually invisible at distances greater than 10 km; thus more flight time was required to locate the plume.

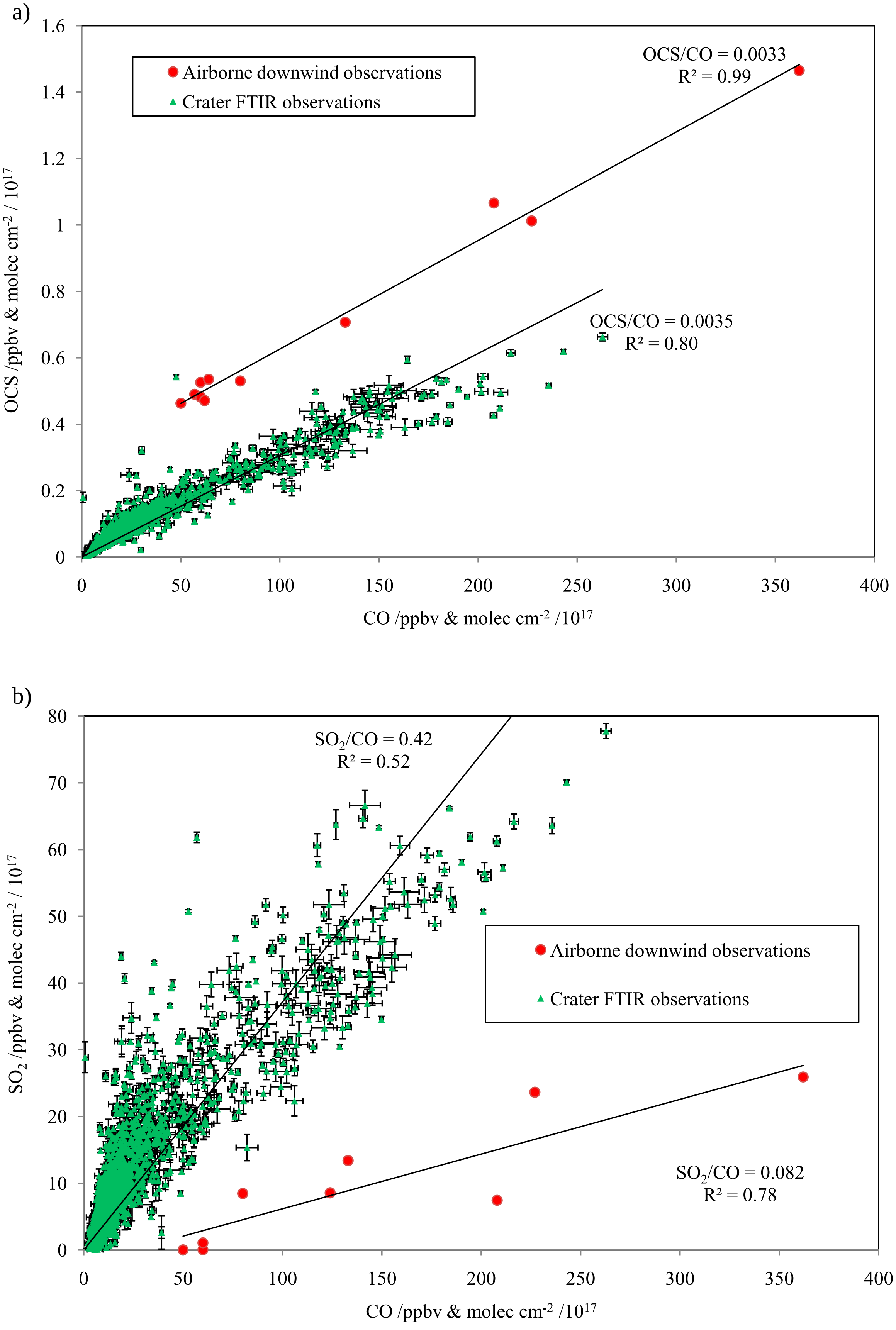
a)
OCS /ppbv & molec cm^{-2} / 10^{17}
CO /ppbv & molec cm^{-2} /10^{17}
0
0.2
0.4
0.6
0.8
1
1.2
1.4
1.6
0
50
100
150
200
250
300
350
400
● Airborne downwind observations
▲ Crater FTIR observations
OCS/CO = 0.0033
R² = 0.99
OCS/CO = 0.0035
R² = 0.80
b)
SO_2 /ppbv & molec cm^{-2} / 10^{17}
CO /ppbv & molec cm^{-2} /10^{17}
0
10
20
30
40
50
60
70
80
0
50
100
150
200
250
300
350
400
SO_2/CO = 0.42
R² = 0.52
● Airborne downwind observations
▲ Crater FTIR observations
SO_2/CO = 0.082
R² = 0.78

Figure 5

Another fall in O_3 to 18.4 ppbv at 2253 UTC is less pronounced but still represents a drop $\sim 2.5\sigma$ below the mean. There is no evidence for O_3 loss in the measurements from flight 8 but we note that SO_2 values measured during this flight never exceeded 20 ppbv.

4. Discussion

4.1. Sulfur Chemistry

[26] The close correspondence of CO and OCS levels (molar OCS/CO ~0.0033–0.0035) based on both airborne and intracrater plume observations provides unambiguous evidence that the ANTCI mission succeeded in sampling the Erebus plume up to 56 km from the source (Figure 3). It further shows that CO and OCS were not appreciably oxidized during the corresponding atmospheric transport (or at least that there was no differential loss of the two species). This result is consistent with their known tropospheric lifetimes (months in the case of CO, years for OCS). By contrast, the SO_2/CO ratio in the distal plume was substantially lower than that observed at the crater (Figure 5b). Although we cannot completely exclude complications arising from calibration differences between the measurements, these results strongly suggest that significant loss of plume SO_2 occurred during transport. Future aircraft studies (with rigorous instrument intercalibration) will be required to confirm this effect and to identify variability that might be associated with atmospheric and meteorological conditions.

[27] It is noteworthy that both the crater rim and distal plume measurements for CO versus OCS are strongly correlated (Figure 5a). This most likely reflects the thermodynamic equilibrium reached for the magmatic conditions prior to emission to the atmosphere and subsquent quenching. In the magmatic gas, the following equilibrium is relevant:

$$3CO + SO_2 \leftrightarrow 2CO_2 + OCS. \tag{1}$$

The CO/CO_2 is fixed according to the oxygen fugacity and temperature of the magma, thus thermodynamically controlling the SO_2/OCS proportion.

[28] A final question addressed that relates to plume sulfur chemistry concerns the source of H_2SO_4 in the Erebus plume. Possible sources of H_2SO_4 could include in situ production within the plume by gas kinetic processes or volatilization of H_2SO_4 from aerosol species where the acid was formed earlier in the young, hot gas mixture leaving the lava lake surface. In the latter case one can hypothesize that this primal H_2SO_4 in a more dilute plume would reach an equilibrium between adsorbed H_2SO_4 on particulates and its gas phase. To address this question, we present calculations here that explore the gas kinetic hypothesis in somewhat greater detail. We begin by accepting the well established three step oxidation process for SO_2 via OH; that is,

$$OH + SO_2 + M \rightarrow HSO_3, \tag{2}$$

$$HSO_3 + O_2 \rightarrow SO_3 + HO_2, \tag{3}$$

$$SO_3 + (H_2O)_2 \rightarrow H_2SO_4 + H_2O. \tag{4}$$

The rate controlling step in this scheme is [2]. Thus, using an upper limit value for measured OH of 4×10^5 cm^{-3} (estimated from limited ANTCI 2005 measurements of OH at 3.8 km above sea level), an average SO_2 plume abundance of 10 ppbv, and a k_2 value of 1×10^{-12} cm^3 $molecule^{-1}$ s^{-1} (estimated for the air temperature at plume altitude), the net formation rate for H_2SO_4 is $\sim 0.8 \times 10^5$ molecule cm^{-3} s^{-1}. Given this value, calculation of the in-plume H_2SO_4 concentration becomes tractable provided the first-order loss of H_2SO_4 to particulates is known. Unfortunately, aerosol parameters were not recorded during our plume intercepts with the Twin Otter. Thus we estimate the aerosol impact based on previous studies by *Eisele and Tanner* [1993] and *Mauldin et al.* [2004]. In this case, the stated loss rates for the different aerosol settings range from 10^{-3} s^{-1} for very clean background conditions to 1 s^{-1} for highly polluted environments. Given the visual appearance of the Erebus plume during our observations (e.g., Figure 2), we consider the intermediate value of $\sim 10^{-2}$ (e.g., typical of the aerosol loading in background continental air) to be the most appropriate [*Eisele and Tanner*, 1993]. Thus, the abundance of H_2SO_4 can be estimated at ~0.4 pptv, a value comparable to that observed in the Erebus plume of 0.1–0.6 pptv. This suggests that the most likely source of in-plume H_2SO_4 was that resulting from gas kinetic processes.

4.2. NO_y Chemistry

[29] Previous observations of high NO_2 abundance above the Erebus crater [*Oppenheimer et al.*, 2005] along with the ANTCI 2005 measurements that reveal the total absence of NO_x in the distal plume (even within 1 km of the crater) strongly suggest that NO_2 formed in the crater is rapidly oxidized during plume transport. Importantly, the detection of HNO_3 and HO_2NO_2 provides further confirmation that NO_2 was present in the very early evolution of the plume.

Figure 5. Comparison of airborne samples (red circles: flights 8 and 9 combined) and intracrater plume sensed by FTIR spectroscopy (green triangles) for (a) CO versus OCS and (b) CO versus SO_2. Note that FTIR measurements represent 8 s averages over a 300 m path, whereas the aircraft measurements are 1 min averages that represent an average over 4 km. The OCS/CO molar ratio (~0.0033–0.0035) is comparable for both proximal and distal plume, while the SO_2 versus CO measurements show that the distal plume is strongly depleted in SO_2. Note the differences in units: volume mixing ratios for the airborne sampling versus column amounts for the retrievals of open-path FTIR spectra. The distal plume data do not plot through the origin but trend to the background tropospheric mixing ratios of CO (~50 ppbv) and OCS (~0.4 ppbv). Note also the tighter correspondence in the aircraft observations between OCS versus CO than for SO_2 versus CO. The scatter in the FTIR-spectra derived SO_2 versus CO plot reflects the dynamics of degassing in the magma conduit [*Oppenheimer et al.*, 2009]. Relative errors shown for FTIR spectra represent ±1σ of the residual for each spectral fit. The spread of values represents plume dilution.

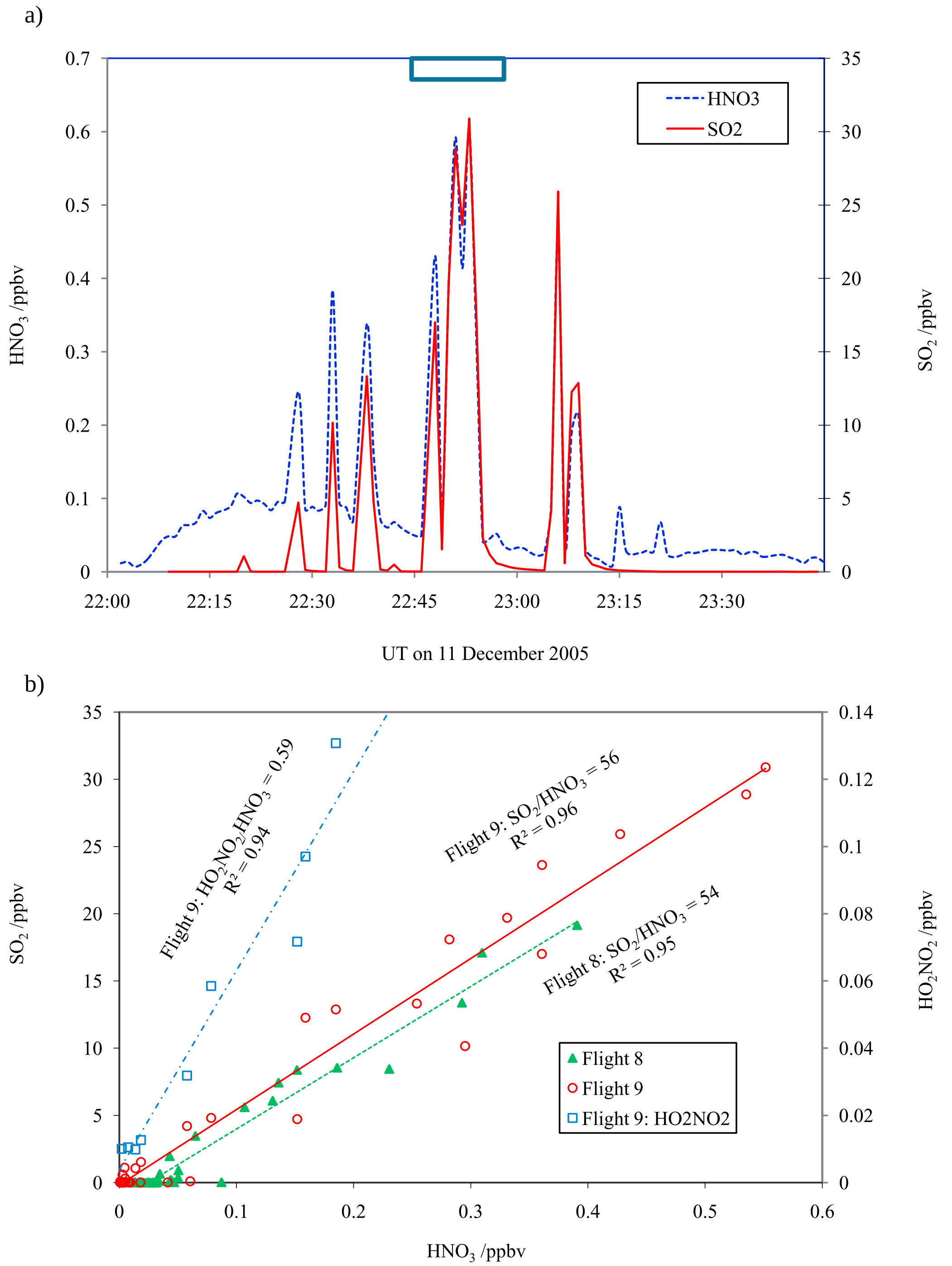

Figure 6. (a) Time profile for flight 9 on 11 December showing correspondence between HNO_3 (dashed blue line) and SO_2 (solid red line) volume mixing ratios. The rectangle indicates the along-plume flight extending up to 56 km downwind from the crater (see Figure 3a). (b) SO_2 versus HNO_3 for flights 8 (green dashed line and triangles) and 9 (red solid line and circles), and HO_2NO_2 versus HNO_3 for flight 9 (blue dash-dotted line with squares).

Stated differently, the observation of highly elevated HNO_3 abundance in the plume is chemically required given the crater observations of highly elevated NO_x along with the absence of NO_x in the downwind plume. The fact that there were elevated levels of HO_2NO_2 in the plume also strongly suggests that the conversion of NO_2 to HNO_3 and HO_2NO_2 occurred in the gas phase, since we know of no heterogeneous process that can generate the thermodynamically unstable HO_2NO_2 species.

[30] Interestingly, the persistence of HO_2NO_2, even out to distances corresponding to a few hours, reflects the low ambient temperatures that were present in the Antarctic

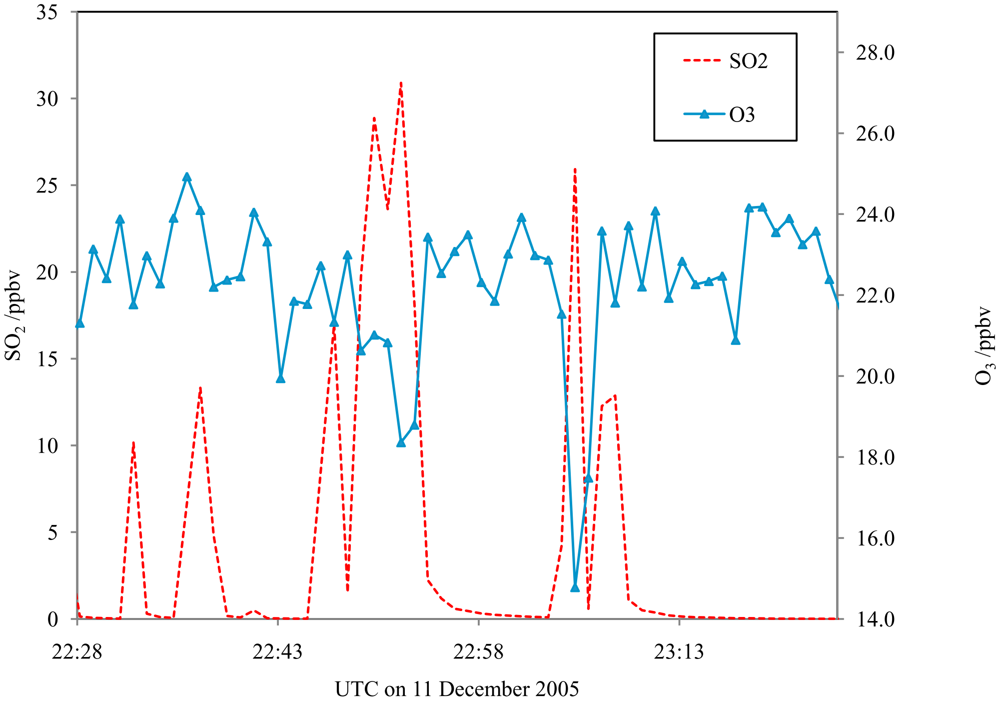

Figure 7. Correspondence between observed SO_2 (red line) and O_3 (blue line with triangles) during part of flight 9. Note depletion of O_3 in two intercepts of the plume involving the highest loadings of SO_2.

atmosphere at that time (~250 K), leading to a relatively low rate of thermal decomposition (e.g., 3–9 h),

$$HO_2NO_2 \rightarrow HO_2 + NO_2. \qquad (5)$$

As far as we are aware, this is the first observation of HO_2NO_2 in a volcanic plume. The HO_2 required in the reaction with NO_2 may have been generated from the hot gas mixture above the lava lake [*Gerlach*, 2004; *Martin et al.*, 2006, 2009] or possibly even by conventional atmospheric photochemical processes involving O_3, CH_2O, or H_2O_2 [e.g., *Finlayson-Pitts and Pitts*, 1997]. For example, high levels of H_2O within the crater in the presence of O_3 and sunlight may have resulted in a major source of HO_x radicals. However, any HO_2 formed in this way would be consumed rather quickly by its reaction either with NO, NO_2 or possibly with halogen species, for example,

$$HO_2 + NO \leftrightarrow NO_2 + OH. \qquad (6)$$

Significant levels of NO most likely were generated by fixation of atmospheric N_2 at the hot lava lake [e.g., *Huebert et al.*, 1999; *Mather et al.*, 2004a] or as a result of mixing of hot magmatic gases and ambient air [*Martin et al.*, 2006]. As noted above, the reaction of NO with HO_2 or halogen oxides would have quickly led to NO_2 formation. The subsequent reaction of this species with either OH or HO_2 radicals would then provide one possible explanation for both the observed HNO_3 and HO_2NO_2; that is,

$$OH + NO_2 + M \rightarrow HNO_3 \qquad (7)$$

$$HO_2 + NO_2 + M \rightarrow HO_2NO_2. \qquad (8)$$

More speculative, is the possibility of generation of elevated HNO_3 via a combination of gas phase and heterogeneous reactions [*Oppenheimer et al.*, 2006; *Roberts et al.*, 2009]:

$$BrO + NO_2 \rightarrow BrONO_2, \qquad (9)$$

$$BrONO_2 + HBr_{(aq)} \leftrightarrow HNO_3 + Br_2, \qquad (10)$$

$$BrONO_2 + H_2O_{(aq)} \leftrightarrow HNO_3 + HOBr. \qquad (11)$$

In 2004, the use of UV differential optical absorption spectroscopy to observe the summit plume rising above the crater indicated a SO_2/NO_2 molar ratio of ~10 [*Oppenheimer et al.*, 2005]. This is substantially lower than the molar ratio of SO_2/HNO_3 that we observe in the core of the distal plume (~56 km) or the observed $SO_2/[HNO_3 + HO_2NO_2]$ ratio of ~40; and suggests that much of the NO_2 observed above the crater was converted into undetected N-bearing species within a short time (<1 h) of exiting the crater. Possibilities include nitrate in the form of aerosol, and/or gas phase halo-nitrates. Indeed, *Radke* [1982] reported nitrate in aerosol sampled 13 km downwind from the crater of Erebus, with a sulfate:nitrate proportion of 9.4:2.2 by mass.

[31] Importantly, there is no evidence for fractionation during transport between gas phase NO_y and SO_2 in the visible summit plume. This is reflected in the stable SO_2/HNO_3 ratio as shown in Figures 6b and 8. Equally significant is the fact that the nitrogen/sulfur results are essentially identical on two days of observations. However, the long-wavelength, "whaleback" profile apparent in the HNO_3 record for flight 9 (Figure 6a) cannot be directly related to the visible plume: it extends cross wind and even upwind of

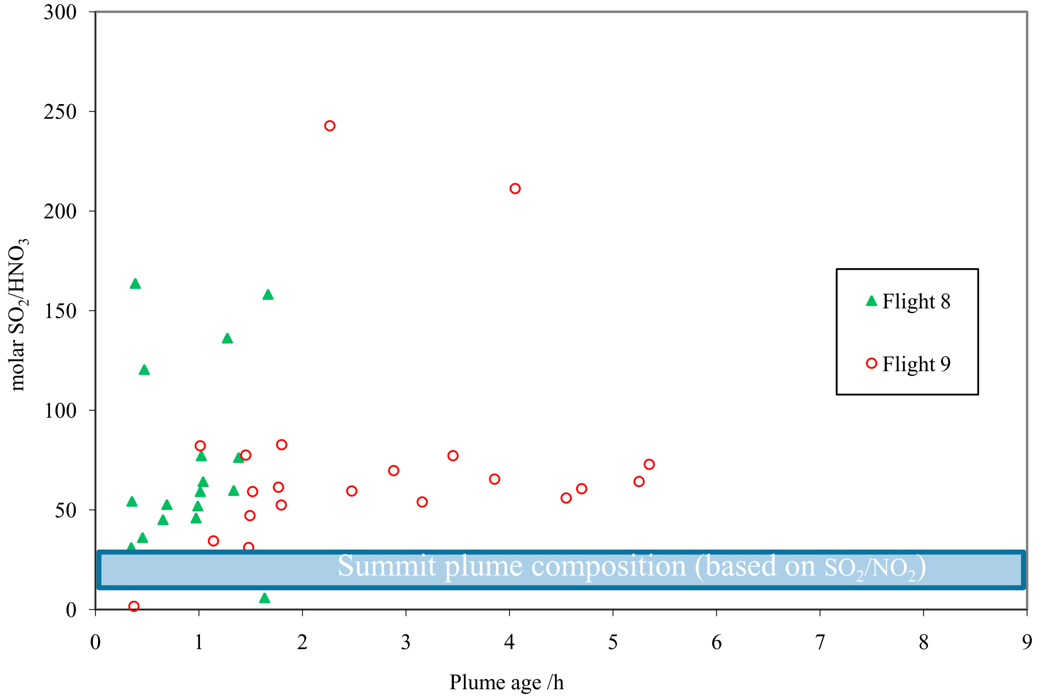

Figure 8. Molar SO_2/HNO_3 ratio plotted versus estimated plume age, for measurements in which SO_2 abundance exceeds 0.05 ppbv.

the crater. There is a similar but less pronounced feature apparent in the HNO_3 measurements for flight 8 but it only extends downwind and more closely envelopes the visible plume. The associated HNO_3 values typically exceed 0.03 ppbv, still substantially above background levels. One interpretation of this phenomenon is that it represents a "pool" of aged plume that accumulated around the volcano as a result of the continuous degassing, comparatively low wind speeds during the two flight days (3.1 and 1.8 m s^{-1} during flights 8 and 9, respectively), and the complex topography of the crater and upper flanks of the volcano, which typically lead to turbulent airflow around the mountain. Still an even more likely scenario is that the longer atmospheric lifetime of HNO_3 versus SO_2 at altitudes above the planetary boundary layer [*Slusher et al.*, 2010] in conjunction with significant fluctuations in wind speed and wind direction during the earlier morning hours preceding the launch of flight 9 (see earlier meteorological discussions, section 2.2) produced the upwind HNO_3 elevations. This would also explain the lack of correlation between SO_2 and HNO_3 in the distributed plume "pool"; that is, SO_2 was lost more rapidly than HNO_3 through chemical conversion to H_2SO_4. In the latter regard, it is significant that even within the visible plume there was some evidence for differential mixing and chemical processing along the fringes of the plume. This is apparent where high values of H_2SO_4 are seen at both very high levels of SO_2 as well as very low.

4.3. Ozone Chemistry

[32] As revealed for flight 9, we see clear evidence of O_3 loss in parts of the Erebus plume but only when SO_2 abundance exceeded ~20 ppbv (Figure 9). (Recall, during flight 8, SO_2 never reached levels in excess of this amount.) There is surprisingly little by way of comparable observations reported in the literature. The identification of near complete O_3 destruction in the plume from the 2000 eruption of Hekla [*Hunton et al.*, 2005; *Millard et al.*, 2006; *Rose et al.*, 2006], while striking, is not comparable to the Erebus observations. The Hekla plume was the result of an explosive eruption, was situated in the stratosphere, and was largely isolated from sunlight in the boreal polar winter. Thus, the Hekla case offers little insight into the chemistry relevant to Erebus volcano.

[33] There are a handful of reports of O_3 loss in tropospheric volcanic plumes. Reporting on the results from airborne measurements in six different volcanic plumes (five of them in Alaska), *Stith et al.* [1978] briefly noted "ozone concentrations were depressed below ambient levels in plumes with relatively high gaseous sulfur," but no further details are provided (even the specific volcanoes are not identified). *Fruchter et al.* [1980] reported an airborne study of the fringes of an ash-rich plume emitted from Mount St. Helens the day after its major explosive eruption of 18 May, 1980. At 200 km from the volcano, they detected H_2S and SO_2 concentrations <100 and <39 ppbv, respectively, and an O_3 abundance that was down by at least a third compared with background values. *Hobbs et al.* [1982] also measured the Mount St. Helens plume, using an instrumented aircraft flying at ~3 km above sea level, and, like *Fruchter et al.* [1980], observed low O_3 levels. In one case, a 'puff' of an ash-rich plume generated by a hydrovolcanic eruption (sampled on 28 March 1980) contained O_3 levels that were just 10% of ambient background abundances. O_3 depletions were recognized on three subsequent missions (between June and September 1980) while the volcano was passively degassing from its lava

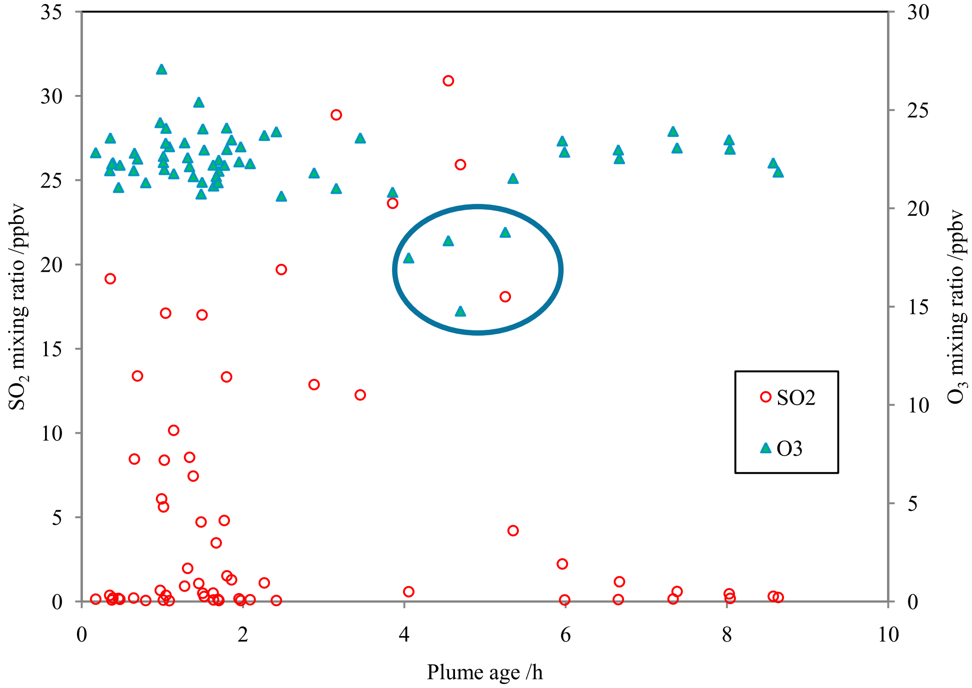

Figure 9. SO_2 (red circles) and O_3 (green triangles) volume mixing ratios as a function of estimated plume age for flights 8 and 9 (only data pairs for which SO_2 exceeded 0.05 ppbv are shown). The circled region highlights observations of low O_3 abundance.

dome. In one of these flights, on 18 June 1980, bromide was identified in the volcanogenic aerosol.

[34] It is significant that all of the above measurements were made prior to the identification of reactive halogens (especially BrO) in volcanic plumes [*Bobrowski et al.*, 2003]. In light of our more recently acquired understanding of the origins and role of reactive halogen chemistry in tropospheric volcanic plumes [*Roberts et al.*, 2009; *von Glasow et al.*, 2009], along with the known presence of bromine species in the aerosol and gas phases in the Erebus plume [*Zreda-Gostynska et al.*, 1997; *Ilyinskaya et al.*, 2010], we consider it likely that reactive bromine was among the key chemical players in the O_3 depletion we observed in the Erebus plume. It is also likely that a significant role was played by preexisting, as well as newly formed aerosol in the Erebus plume. Although no aerosol measurements were made during this study, we expect that the very elevated levels of SO_2 were accompanied by correspondingly elevated aerosol abundance. This would have provided a heterogeneous pathway for the production of reactive halogens via the formation and release of gas phase Br_2, which then would photolyze to form 2 Br, leading to a reaction with O_3 to form 2 BrO. The most likely reaction of BrO (e.g., in the absence of plume NO_x) would be with HO_2 radicals thereby generating HOBr, thus leading to an autocatalytic cycle that would rapidly destroy O_3 [*Oppenheimer et al.*, 2006; *Bobrowski et al.*, 2007; *Roberts et al.*, 2009]. This then points to the removal of NO_2 from the plume as a critical step in that it is this species that most frequently leads to chain termination of BrO or ClO by forming the corresponding nitrate species [*McElroy et al.*, 1992; *Schoeberl et al.*, 1993]. Even if the latter were formed, however, in the case of the Erebus plume, the species $BrONO_2$ and/or $ClONO_2$ could also initiate O_3 destruction via direct photolysis (e.g., for mid-December the two channels for $ClONO_2$, J_{tot} is 4.3×10^{-5} s^{-1} at high noon and that for $BrONO_2$ is 1×10^{-3} s^{-1}).

[35] But why did ozone loss not show up in all the Erebus plume transects? The answer most likely has to do with the effect of aerosols. As previously stated, excessively high levels of aerosols make possible the generation of reactive halogen species. It seems reasonable that some of the highest aerosol loadings for the plume would coincide with some of the highest SO_2 concentrations, thereby leading to the highest reactive halogen production and O_3 loss.

5. Conclusions

[36] We detected the magmatic gases SO_2, CO and OCS in the distal Erebus plume, as expected from ground-based measurements by FTIR spectroscopy. The OCS/CO molar ratio (~0.0033) in the distal plume (up to a plume age estimated at ~5 h) corresponds very closely with the intracrater composition, consistent with the relatively long lifetimes of these species ($\gg$months). By contrast, the SO_2/CO ratio in the distal core plume (aged >1 h) is around one fifth that of the intracrater plume. However, the aircraft measurements suggest that if a major heterogeneous loss in SO_2 did occur, it took place near the crater itself, and most likely involved conversion via "cloud processing" in liquid phase aerosol in the proximal plume.

[37] We have convincingly shown that nitrogen is a key component of the Erebus plume. We identified both HNO_3 and HO_2NO_2 in the plume, consistent with the previous identification of large quantities of NO_x directly above the Erebus crater [*Oppenheimer et al.*, 2005] but the absence of

NO_x in the downwind plume. HNO_3 and HO_2NO_2 represent oxidation products of NO_x formed initially through thermal fixation of atmospheric molecular nitrogen close to the hot lava lake surface. However, the combined HNO_3 and HO_2NO_2 abundance measured was found to be less than a tenth of that expected based on the CO/NO_2 ratio measured in 2003. This suggests that additional N-bearing species might have been present in the distal plume either in the form of the halogen species $ClONO_2$, and $BrONO_2$, or as aerosol nitrates. We also identified a "pool" of aged plume abundant in HNO_3 and with elevated H_2SO_4 levels but depleted in SO_2, which extended around the summit, separate from the visible crater plume. We believe this "pool" accumulated either through the steady degassing of the volcano and separation and stagnation of parts of the plume or as a result of shifts in wind speed and direction hours before the launching of the Erebus flights and outside of the small temporal sampling window of the rawinsonde wind observations.

[38] We identified significant O_3 loss in some of the plume transects. In one case, O_3 abundance was ~35% of ambient levels. This is likely the result of reactive halogen (especially Br) chemistry, which could have been initiated by heterogeneous processes given that the key ingredients are known to have been present (bromine, sunlight and acid aerosol [e.g., *Roberts et al.*, 2009]). Firm objectives for future work on Erebus are to determine if and when BrO is present in the plume using UV spectroscopy, and to model the chemistry of an Erebus-like plume containing reactive nitrogen and halogen species as well as an assortment of aerosol species. We emphasize that plumes can be complex, particularly with respect to their mixing dynamics.

[39] We also encourage future airborne campaigns including both crewed aircraft and unmanned aerial vehicles, as these are likely to shed further light on the critical chemical and physical processes occurring in the plume, leading to improved understanding of the nature and extent of the impact of Erebus emissions on the atmospheric and cryospheric environments. In particular, future work should be undertaken to characterize the aerosol phase in the downwind plume, and to trace the plume over greater distances (hundreds of km). That this should prove fruitful is strongly suggested by a subset of the measurements made during the ANTCI 2005 field study, which revealed remnants of the Erebus plume ~600 km from the volcano [*Slusher et al.*, 2010]. Thus, we propose that far more ambitious airborne plume studies of Erebus are warranted in the future.

[40] **Acknowledgments.** This work was generously supported by grants from the Office of Polar Programs, National Science Foundation, to P.R.K. and D.D. and by a "study abroad fellowship" awarded to C.O. by the Leverhulme Trust. C.O. also acknowledges support from the EU Framework 6 project "NOVAC" and the NERC National Centre for Earth Observation. D.D. is grateful to William Neff for his retrieval of MET data used to help characterize plume drift velocity, to Darlene Slusher for her efforts in drafting early versions of several figures and providing modifications to these, and to several students and technicians who contributed to the data collection process, namely, Will Wallace and Ed Kosciuch. We thank the three referees for thorough reviews, Yinon Rudich for editorial evaluation and advice, Tjarda Roberts, Rob Martin, Rod Jones, and Tony Cox for discussions, and Mike Burton for providing the FTIR spectral retrieval code.

References

Arimoto, R., A. Hogan, P. Grube, D. Davis, J. Webb, C. Schloesslin, S. Sage, and F. Raccah (2004a), Major ions and radionuclides in aerosol particles from the South Pole during ISCAT-2000, *Atmos. Environ.*, *38*, 5473–5484, doi:10.1016/j.atmosenv.2004.01.049.

Arimoto, R., C. Schloesslin, D. Davis, A. Hogan, P. Grube, W. Fitzgerald, and C. Lamborg (2004b), Lead and mercury in aerosol particles collected over the South Pole during ISCAT-2000, *Atmos. Environ.*, *38*, 5485–5491, doi:10.1016/j.atmosenv.2004.03.073.

Bobrowski, N., and U. Platt (2007), SO_2/BrO ratios studied in five volcanic plumes, *J. Volcanol. Geotherm. Res.*, *166*, 147–160, doi:10.1016/j.jvolgeores.2007.07.003.

Bobrowski, N., G. Hönninger, B. Galle, and U. Platt (2003), Detection of bromine monoxide in a volcanic plume, *Nature*, *423*, 273–276, doi:10.1038/nature01625.

Bobrowski, N., R. von Glasow, A. Aiuppa, S. Inguaggiato, I. Louban, O. W. Ibrahim, and U. Platt (2007), Reactive halogen chemistry in volcanic plumes, *J. Geophys. Res.*, *112*, D06311, doi:10.1029/2006JD007206.

Burton, M. R., C. Oppenheimer, L. A. Horrocks, and P. W. Francis (2000), Remote sensing of CO_2 and H_2O emission rates from Masaya volcano, Nicaragua, *Geology*, *28*, 915–918, doi:10.1130/0091-7613(2000)28<915:RSOCAH>2.0.CO;2.

Chin, M., and D. J. Jacob (1996), Anthropogenic and natural contributions to tropospheric sulfate: A global model analysis, *J. Geophys. Res.*, *101*(D13), 18,691–18,699, doi:10.1029/96JD01222.

Chuan, R. L. (1994), Dispersal of volcano-derived particles from Mount Erebus in the Antarctic atmosphere, in *Volcanological and Environmental Studies of Mount Erebus, Antarctica*, *Antarct. Res. Ser.*, vol. 66, edited by P. R. Kyle, pp. 97–102, AGU, Washington, D. C.

Chuan, R. L., J. Palais, W. I. Rose, and P. R. Kyle (1986), Fluxes, sizes, morphology and compositions of particles in the Mt. Erebus volcanic plume, December 1983, *J. Atmos. Chem.*, *4*, 467–477, doi:10.1007/BF00053846.

Davis, D., et al. (2001), Unexpected high levels of NO observed at South Pole, *Geophys. Res. Lett.*, *28*(19), 3625–3628, doi:10.1029/2000GL012584.

Davis, D. D., et al. (2004), An overview of ISCAT 2000, *Atmos. Environ.*, *38*, 5363–5373, doi:10.1016/j.atmosenv.2004.05.037.

Davis, D. D., et al. (2008), A reassessment of Antarctic plateau reactive nitrogen based on ANTCI 2003 airborne and ground based measurements, *Atmos. Environ.*, *42*, 2831–2848, doi:10.1016/j.atmosenv.2007.07.039.

Edwards, D. J., and A. Dudhia (1996), Reference forward model: High level algorithms definition, *ESA Doc. PO-MA-OXF-GS-0004*, Eur. Space Agency, Paris.

Eisele, F. L., and D. J. Tanner (1993), Measurement of the gas phase concentration of H_2SO_4 and methane sulfonic acid and estimates of H_2SO_4 production and loss in the atmosphere, *J. Geophys. Res.*, *98*(D5), 9001–9010, doi:10.1029/93JD00031.

Finlayson-Pitts, B. J., and J. N. Pitts (1997), Tropospheric air pollution: Ozone, airborne toxics, polycyclic aromatic hydrocarbons, and particles, *Science*, *276*, 1045–1052, doi:10.1126/science.276.5315.1045.

Fruchter, J. S., et al. (1980), Mount St. Helens ash from the 18 May 1980 eruption: Chemical, physical, mineralogical and biological properties, *Science*, *209*, 1116–1125, doi:10.1126/science.209.4461.1116.

Gerlach, T. M. (2004), Volcanic sources of tropospheric ozone-depleting trace gases, *Geochem. Geophys. Geosyst.*, *5*, Q09007, doi:10.1029/2004GC000747.

Graf, H.-F., J. Feichter, and B. Langmann (1997), Volcanic sulfur emissions: Estimates of source strength and its contribution to the global sulfate distribution, *J. Geophys. Res.*, *102*(D9), 10,727–10,738, doi:10.1029/96JD03265.

Graf, H.-F., S. V. Shirsat, C. Oppenheimer, M. J. Jarvis, R. Podzun, and D. Jacob (2009), Continental scale Antarctic deposition of sulphur and black carbon from anthropogenic and volcanic sources, *Atmos. Chem. Phys. Discuss.*, *9*, 26,577–26,592.

Gregory, G. L., C. L. Hudgins, and R. A. Edahl (1983), Laboratory evaluation of an airborne ozone instrument which compensates for altitude/sensitivity effects, *Environ. Sci. Technol.*, *17*, 100–103, doi:10.1021/es00108a007.

Gregory, G. L., J. M. Hoell Jr., A. L. Torres, M. A. Carroll, B. A. Ridley, M. O. Rodgers, J. Bradshaw, S. Sandholm, and D. D. Davis (1990), An intercomparison of airborne nitric oxide measurements: A second opportunity, *J. Geophys. Res.*, *95*(D7), 10,129–10,138, doi:10.1029/JD095iD07p10129.

Hobbs, P. V., J. P. Tuell, D. A. Hegg, L. F. Radke, and M. W. Eltgroth (1982), Particles and gases in the emissions from the 1980–1981 volcanic eruptions of Mt. St. Helens, *J. Geophys. Res.*, *87*(C13), 11,062–11,086, doi:10.1029/JC087iC13p11062.

Hoell, J. M., Jr., G. L. Gregory, D. S. McDougal, G. W. Sachse, G. F. Hill, E. P. Condon, and R. A. Rasmussen (1987), Airborne intercomparison of carbon monoxide measurement techniques, *J. Geophys. Res.*, *92*(D2), 2009–2019, doi:10.1029/JD092iD02p02009.

Horrocks, L. A., C. Oppenheimer, M. R. Burton, H. J. Duffell, N. M. Davies, N. A. Martin, and W. Bell (2001), Open-path Fourier transform infrared spectroscopy of SO_2: An empirical error budget analysis, with implications for volcano monitoring, *J. Geophys. Res.*, *106*(D21), 27,647–27,659, doi:10.1029/2001JD000343.

Huebert, B., P. Vitousek, J. Sutton, T. Elias, J. Heath, S. Coeppicus, S. Howell, and B. Blomquist (1999), Volcano fixes nitrogen into plant-available forms, *Biogeochemistry*, *47*, 111–118.

Huey, L. G., D. R. Hanson, and C. J. Howard (1995), Reactions of SF_6^- and I^- with atmospheric trace gases, *J. Phys. Chem.*, *99*, 5001–5008, doi:10.1021/j100014a021.

Huey, L. G., et al. (2004), CIMS measurements of HNO_3 and SO_2 at the South Pole during ISCAT 2000, *Atmos. Environ.*, *38*, 5411–5421, doi:10.1016/j.atmosenv.2004.04.037.

Hunton, D. E., et al. (2005), In-situ aircraft observations of the 2000 Mt. Hekla volcanic cloud: Composition and chemical evolution in the Arctic lower stratosphere, *J. Volcanol. Geotherm. Res.*, *145*, 23–34, doi:10.1016/j.jvolgeores.2005.01.005.

Ilyinskaya, E., C. Oppenheimer, T. A. Mather, R. S. Martin, and P. R. Kyle (2010), Size-resolved chemical composition of aerosol emitted by Erebus volcano, Antarctica., *Geochem. Geophys. Geosyst.*, doi:10.1029/2009GC002855, in press.

Martin, R. S., T. A. Mather, and D. M. Pyle (2006), High-temperature mixtures of magmatic and atmospheric gases, *Geochem. Geophys. Geosyst.*, *7*, Q04006, doi:10.1029/2005GC001186.

Martin, R. S., T. J. Roberts, T. A. Mather, and D. M. Pyle (2009), The implications of H_2S and H_2 kinetic stability in high-T mixtures of magmatic and atmospheric gases for the production of oxidized trace species (e.g., BrO and NO_x), *Chem. Geol.*, *263*, 143–150, doi:10.1016/j.chemgeo.2008.12.028.

Mather, T. A., A. G. Allen, D. M. Pyle, B. M. Davison, C. Oppenheimer, and A. J. S. McGonigle (2004a), Nitric acid from volcanoes, *Earth Planet. Sci. Lett.*, *218*, 17–30, doi:10.1016/S0012-821X(03)00640-X.

Mather, T. A., D. M. Pyle, and A. G. Allen (2004b), Volcanic source for fixed nitrogen in the early Earth's atmosphere, *Geology*, *32*, 905–908, doi:10.1130/G20679.1.

Mauldin, R. L., III, L. Frost, G. J. Chen, G. Tanner, D. J. Prevot, A. S. H. Davis, and D. D. Eisele (1998), OH measurements during the First Aerosol Characterization Experiment (ACE 1): Observations and model comparisons, *J. Geophys. Res.*, *103*(D13), 16,713–16,729, doi:10.1029/98JD00882.

Mauldin, R. L., III, E. Kosciuch, B. Henry, F. L. Eisele, R. Shetter, B. Lefer, G. Chen, D. Davis, G. Huey, and D. Tanner (2004), Measurements of OH, HO_2 +RO_2, H_2SO_4, and MSA at the South Pole during ISCAT 2000, *Atmos. Environ.*, *38*, 5423–5437, doi:10.1016/j.atmosenv.2004.06.031.

McElroy, M. B., R. J. Salawitch, and K. Minschwaner (1992), The changing stratosphere, *Planet. Space Sci.*, *40*, 373–401, doi:10.1016/0032-0633(92)90070-5.

Millard, G. A., T. A. Mather, D. M. Pyle, W. I. Rose, and B. Thornton (2006), Halogen emissions from a small volcanic eruption: Modeling the peak concentrations, dispersion, and volcanically induced ozone loss in the stratosphere, *Geophys. Res. Lett.*, *33*, L19815, doi:10.1029/2006GL026959.

Oppenheimer, C., and P. R. Kyle (2008), Probing the magma plumbing of Erebus volcano, Antarctica, by open-path FTIR spectroscopy of gas emissions, *J. Volcanol. Geotherm. Res.*, *177*, 743–754, doi:10.1016/j.jvolgeores.2007.08.022.

Oppenheimer, C., P. Francis, M. Burton, A. Maciejewski, and L. Boardman (1998), Remote measurement of volcanic gases by Fourier transform infrared spectroscopy, *Appl. Phys. B*, *67*, 505–515, doi:10.1007/s003400050536.

Oppenheimer, C., P. R. Kyle, V. I. Tsanev, A. J. S. McGonigle, T. A. Mather, and D. Sweeney (2005), Mt. Erebus, the largest point source of NO_2 in Antarctica, *Atmos. Environ.*, *39*, 6000–6006, doi:10.1016/j.atmosenv.2005.06.036.

Oppenheimer, C., V. I. Tsanev, C. F. Braban, R. A. Cox, J. W. Adams, A. Aiuppa, N. Bobrowski, P. Delmelle, J. Barclay, and A. J. S. McGonigle (2006), BrO formation in volcanic plumes, *Geochim. Cosmochim. Acta*, *70*, 2935–2941, doi:10.1016/j.gca.2006.04.001.

Oppenheimer, C., A. S. Lomakina, P. R. Kyle, N. G. Kingsbury, and M. Boichu (2009), Pulsatory magma supply to a phonolite lava lake, *Earth Planet. Sci. Lett.*, *284*, 392–398, doi:10.1016/j.epsl.2009.04.043.

Radke, L. F. (1982), Sulphur and sulphate from Mt Erebus, *Nature*, *299*, 710–712, doi:10.1038/299710a0.

Roberts, T. J., C. F. Braban, R. S. Martin, C. Oppenheimer, J. W. Adams, R. A. Cox, R. L. Jones, and P. T. Griffiths (2009), Formation of BrO and ClO_x in volcanic plumes and chemical impacts on O_3, *Chem. Geol.*, *263*, 151–163, doi:10.1016/j.chemgeo.2008.11.012.

Rodgers, C. D. (1976), Retrieval of atmospheric temperature and composition from remote measurements of thermal radiation, *Rev. Geophys.*, *14*(4), 609–624, doi:10.1029/RG014i004p00609.

Rose, W. I., R. L. Chuan, and P. R. Kyle (1985), Rate of sulphur dioxide emission from Erebus volcano, Antarctica, December 1983, *Nature*, *316*, 710–712, doi:10.1038/316710a0.

Rose, W. I., et al. (2006), Atmospheric chemistry of a 33–34 hour old volcanic cloud from Hekla volcano (Iceland): Insights from direct sampling and the application of chemical box modeling, *J. Geophys. Res.*, *111*, D20206, doi:10.1029/2005JD006872.

Rothman, L. S., et al. (2005), The HITRAN 2004 molecular spectroscopic database, *J. Quant. Spectrosc. Radiat. Transfer*, *96*, 139–204, doi:10.1016/j.jqsrt.2004.10.008.

Schoeberl, M. R., et al. (1993), The evolution of CLO and NO along air parcel trajectories, *Geophys. Res. Lett.*, *20*(22), 2511–2514, doi:10.1029/93GL01690.

Shaw, G. E. (1983), X-ray spectrometry of polar aerosols, *Atmos. Environ.*, *17*, 329–339, doi:10.1016/0004-6981(83)90049-5.

Shirsat, S. V., and H.-F. Graf (2009), An emission inventory of sulfur from anthropogenic sources in Antarctica, *Atmos. Chem. Phys.*, *9*, 3397–3408.

Slusher, D. L., S. J. Pitteri, B. J. Haman, D. J. Tanner, and L. G. Huey (2001), A chemical ionization technique for measurement of pernitric acid in the upper troposphere and the polar boundary layer, *Geophys. Res. Lett.*, *28*(20), 3875–3878, doi:10.1029/2001GL013443.

Slusher, D. L., et al. (2010), Atmospheric chemistry results from the ANTCI 2005 Antarctic Plateau Airborne Study, *J. Geophys. Res.*, doi:10.1029/2009JD012605, in press.

Stevenson, D. S., C. E. Johnson, W. I. Collins, and R. G. Derwent (2003), The tropospheric sulphur cycle and the role of volcanic SO_2, in *Volcanic Degassing*, edited by C. Oppenheimer, D. M. Pyle, and J. Barclay, *Geol. Soc. Spec. Publ.*, *213*, 295–305.

Stith, J. L., P. V. Hobbs, and L. F. Radke (1978), Airborne particle and gas measurements in the emissions from six volcanoes, *J. Geophys. Res.*, *83*(C8), 4009–4017, doi:10.1029/JC083iC08p04009.

Tanner, D. J., A. Jefferson, and F. L. Eisele (1997), Selected ion chemical ionization mass spectrometric measurement of OH, *J. Geophys. Res.*, *102*(D5), 6415–6425, doi:10.1029/96JD03919.

Theys, N., M. Van Roozendael, B. Dils, F. Hendrick, N. Hao, and M. De Mazière (2009), First satellite detection of volcanic bromine monoxide emission after the Kasatochi eruption, *Geophys. Res. Lett.*, *36*, L03809, doi:10.1029/2008GL036552.

Vallelonga, P., J.-P. Candelone, K. Van de Velde, M. A. J. Curran, V. I. Morgan, and K. J. R. Rosman (2003), Lead, Ba and Bi in Antarctic Law Dome ice corresponding to the 1815 AD Tambora eruption: An assessment of emission sources using Pb isotopes, *Earth Planet. Sci. Lett.*, *211*, 329–341, doi:10.1016/S0012-821X(03)00208-5.

von Glasow, R., N. Bobrowski, and C. Kern (2009), The effects of volcanic eruptions on atmospheric chemistry, *Chem. Geol.*, *263*, 131–142, doi:10.1016/j.chemgeo.2008.08.020.

Zreda-Gostynska, G., P. R. Kyle, D. Finnegan, and K. M. Prestbo (1997), Volcanic gas emissions from Mount Erebus and their impact on the Antarctic environment, *J. Geophys. Res.*, *102*(B7), 15,039–15,055, doi:10.1029/97JB00155.

A. Beyersdorf and J. Crawford, NASA Langley Research Center, MS 483, Hampton, VA 23681, USA.

D. Blake, Department of Chemistry, University of California, 516 Rowland Hall, Irvine, CA 92697, USA.

M. Buhr, Air Quality Design, Inc., Ste. B, 801 Brickyard Cir., Golden, CO 80403, USA.

D. Davis, G. Huey, S. Kim, and D. Tanner, School of Earth and Atmospheric Sciences, Georgia Institute of Technology, 311 Ferst Dr., Atlanta, GA 30332-0340, USA.

F. Eisele and L. Mauldin, Atmospheric Chemistry Division, National Center for Atmospheric Research, 1850 Table Mesa Dr., Boulder, CO 80305, USA.

P. Kyle, Department of Earth and Environmental Science, New Mexico Institute of Mining and Technology, 801 Leroy Pl., Socorro, NM 87801, USA.

C. Oppenheimer, Department of Geography, University of Cambridge, Downing Pl., Cambridge CB2 3EN, UK. (co200@cam.ac.uk)